Published in final edited form as:
Cell Tissue Res. 2012 March ; 347(3): 575–588. doi:10.1007/s00441-011-1197-3.

Synthetic scaffold coating with adeno-associated virus encoding BMP2 to promote endogenous bone repair

Kenneth M. Dupont,
Parker H. Petit Institute for Bioengineering and Bioscience, Georgia Institute of Technology, 315 Ferst Drive, Atlanta, GA 30332, USA. George W. Woodruff School of Mechanical Engineering, Georgia Institute of Technology, 315 Ferst Drive, Atlanta, GA 30332, USA. Exponent Failure Analysis Associates, 3401 Market Street, Suite 300, Philadelphia, PA 19104, USA

Joel D. Boerckel,
Parker H. Petit Institute for Bioengineering and Bioscience, Georgia Institute of Technology, 315 Ferst Drive, Atlanta, GA 30332, USA. George W. Woodruff School of Mechanical Engineering, Georgia Institute of Technology, 315 Ferst Drive, Atlanta, GA 30332, USA

Hazel Y. Stevens,
Parker H. Petit Institute for Bioengineering and Bioscience, Georgia Institute of Technology, 315 Ferst Drive, Atlanta, GA 30332, USA. George W. Woodruff School of Mechanical Engineering, Georgia Institute of Technology, 315 Ferst Drive, Atlanta, GA 30332, USA

Tamim Diab,
Parker H. Petit Institute for Bioengineering and Bioscience, Georgia Institute of Technology, 315 Ferst Drive, Atlanta, GA 30332, USA. George W. Woodruff School of Mechanical Engineering, Georgia Institute of Technology, 315 Ferst Drive, Atlanta, GA 30332, USA

Yash M. Kolambkar,
Parker H. Petit Institute for Bioengineering and Bioscience, Georgia Institute of Technology, 315 Ferst Drive, Atlanta, GA 30332, USA. Wallace H. Coulter Department of Biomedical Engineering, Georgia Institute of Technology, 315 Ferst Drive, Atlanta, GA 30332, USA

Masahiko Takahata,
Center for Musculoskeletal Research, School of Medicine and Dentistry, University of Rochester, 601 Elmwood Avenue, Box 665, Rochester, NY 14642, USA

Edward M. Schwarz, and
Center for Musculoskeletal Research, School of Medicine and Dentistry, University of Rochester, 601 Elmwood Avenue, Box 665, Rochester, NY 14642, USA

Robert E. Guldberg
Parker H. Petit Institute for Bioengineering and Bioscience, Georgia Institute of Technology, 315 Ferst Drive, Atlanta, GA 30332, USA. George W. Woodruff School of Mechanical Engineering, Georgia Institute of Technology, 315 Ferst Drive, Atlanta, GA 30332, USA. Wallace H. Coulter Department of Biomedical Engineering, Georgia Institute of Technology, 315 Ferst Drive, Atlanta, GA 30332, USA

Kenneth M. Dupont: kennethmdupont@yahoo.com; Robert E. Guldberg: robert.guldberg@me.gatech.edu

Abstract

Correspondence to: Robert E. Guldberg, robert.guldberg@me.gatech.edu.

Biomaterial scaffolds functionalized to stimulate endogenous repair mechanisms via the incorporation of osteogenic cues offer a potential alternative to bone grafting for the treatment of large bone defects. We first quantified the ability of a self-complementary adeno-associated viral vector encoding bone morphogenetic protein 2 (scAAV2.5-BMP2) to enhance human stem cell osteogenic differentiation in vitro. In two-dimensional culture, scAAV2.5-BMP2-transduced human mesenchymal stem cells (hMSCs) displayed significant increases in BMP2 production and alkaline phosphatase activity compared with controls. hMSCs and human amniotic-fluid-derived stem cells (hAFS cells) seeded on scAAV2.5-BMP2-coated three-dimensional porous polymer Poly(ε-caprolactone) (PCL) scaffolds also displayed significant increases in BMP2 production compared with controls during 12 weeks of culture, although only hMSC-seeded scaffolds displayed significantly increased mineral formation. PCL scaffolds coated with scAAV2.5-BMP2 were implanted into critically sized immunocompromised rat femoral defects, both with or without pre-seeding of hMSCs, representing ex vivo and in vivo gene therapy treatments, respectively. After 12 weeks, defects treated with acellular scAAV2.5-BMP2-coated scaffolds displayed increased bony bridging and had significantly higher bone ingrowth and mechanical properties compared with controls, whereas defects treated with scAAV2.5-BMP2 scaffolds pre-seeded with hMSCs failed to display significant differences relative to controls. When pooled, defect treatment with scAAV2.5-BMP2-coated scaffolds, both with or without inclusion of pre-seeded hMSCs, led to significant increases in defect mineral formation at all time points and increased mechanical properties compared with controls. This study thus presents a novel acellular bone-graft-free endogenous repair therapy for orthotopic tissue-engineered bone regeneration.

Keywords

Synthetic scaffold; Large bone defect; Self-complementary adeno-associated virus (scAAV); Bone morphogenetic protein-2 (BMP2); Stem cells; Human

Introduction

Large bone defects and fracture nonunions present a significant clinical challenge affecting large numbers of patients and resulting in high costs (Werntz et al. 1996). In such defects, healing may be limited by a variety of factors such as soft tissue damage, loss of vascularity, distraction of fracture fragments, soft-tissue interposition, malnutrition, infection, instability, periosteal stripping, and systemic diseases such as diabetes and rheumatoid arthritis (Tseng et al. 2008; Kalfas 2001). Lack of healing creates a need for surgical intervention, with over 500,000 bone-grafting operations performed annually in the United States for patients with nonunions or large defects (Bucholz 2002).

Autografts are the current gold standard for treatment of large bone defects (Tseng et al. 2008); however, the use of autografts is associated with numerous limitations including limited graft availability, donor site morbidity as high as 10%–30%, the potential for injury to nerves and blood vessels during harvesting, and the risk of possible infection (Younger and Chapman 1989). Therefore, devitalized cadaveric allograft bone is often used because of its more ready availability; however, this material displays limited integration with host bone resulting in as many as 1/3 of these grafts failing within 2–3 years after implantation (Berrey et al. 1990).

Schwarz and colleagues have recently developed a novel method for increasing allograft integration with host bone in a murine large-bone-defect model through gene therapy treatment; this treatment consists of coating allografts with an adeno-associated viral vector (AAV) encoding factors that promote allograft repair (Ito et al. 2005; Koefoed et al. 2005; Awad et al. 2007). In particular, Yazici et al. (2011) have recently reported enhancement of

allograft healing after coating the allograft with self-complementary AAV (scAAV) delivering the gene encoding bone morphogenetic protein 2 (BMP2), a potent osteogenic protein that promotes migration, proliferation, and osteogenic differentiation of stem cells (Wozney and Rosen 1998; Chen et al. 2004). Recombinant human BMP2 (rhBMP2) has been used to increase the healing of critically sized defects in rabbit, sheep, dog, and rat models (Yasko et al. 1992; Lee et al. 1994; Oest et al. 2007; Ohura et al. 1999; Kolambkar et al. 2010), and success in clinical trials has led the US Food and Drug Administration (FDA) to approve application of rhBMP2 on absorbable collagen sponges for single-level interbody fusions of the lumbar spine (InFuse—Medtronic; Einhorn 2003). However, concern is growing over delivering osteogenic signaling cues through bolus delivery of large doses of recombinant protein, because of side effects such as inflammation and ectopic bone formation, which are associated with the large doses of delivered protein needed for improved repair (Cahill et al. 2009).

Delivery of BMP2 signals through gene therapy vectors presents an alternative to bolus delivery of large quantities of recombinant protein. The adeno-associated virus possesses many qualities that make it an attractive viral vector choice. These include the absence of host inflammatory or cell-mediated immune responses and its abilities to transduce a broad range of cells including musculoskeletal cells, to infect dividing and non-dividing cells, and to deliver long-term gene expression in cell types that have relatively long lifetimes, such as osteocytes or muscle cells, thus providing enhanced opportunities for endogenous repair (Schwarz 2000).

Whereas Yazici et al. (2011) have reported that scAAV-BMP2-coated allografts can heal defects comparably to autograft treatment, allograft treatment still poses some drawbacks, including the possibility of disease transmission (Mroz et al. 2008) and a lack of porosity throughout the cortices, thus limiting vascular invasion. Additionally, the nonporous cortical surfaces of allograft bone prohibit the uniform distribution of coated AAV particles (Yazici et al. 2008). Synthetic scaffolds present an alternative structure for scAAV-BMP2 particle delivery by providing a greater surface area and lower risk of immunogenicity or disease transmission (Saito et al. 2005). Porous poly(ε-caprolactone) (PCL) polymer scaffolds have been shown to be an effective scaffold for multiple bone tissue engineering applications (Wojtowicz et al. 2010; Hutmacher 2000). These scaffolds, formed through fused deposition modeling, feature three-dimensional porous structures of reproducible and scalable geometry allowing cell attachment/proliferation and vascular invasion. They have mechanical properties similar to those of trabecular bone and are biocompatible/bioresorbable, and the PCL material has received FDA approval for use in numerous medical devices. We have recently used these PCL scaffolds as a delivery vehicle for human stem cells to enhance the healing of critically sized immunodeficient rat femoral defects (Dupont et al. 2010), although cell-mediated treatment alone does not achieve functional restoration, suggesting the need for additional osteogenic stimuli (Burastero et al. 2010; Rai et al. 2004).

In this study, we first hypothesized that the delivery of scAAV-BMP2-coated PCL scaffolds to segmental defect sites (in vivo gene therapy in which host cells are transduced) would enhance endogenous repair of critically sized rat femoral defects compared with treatment with control AAV-Luciferase (AAV-Luc)-coated scaffolds. Secondly, we hypothesized that delivery of genetically modified stem cells programmed toward osteogenic differentiation by pre-culture on scAAV-BMP2-coated PCL scaffolds (ex vivo gene transfer in which a specific set of cells are transduced outside of the host) would further enhance defect healing. These hypotheses were tested by using an in vivo critically sized rat femoral defect model, with analysis methods including quantitative micro-computed tomography (micro-CT) imaging and biomechanical testing.

Materials and methods

PCL scaffold preparation/AAV coating

PCL cylindrical scaffolds (9 mm in height, 5 mm in diameter, and 85% porosity) were punched from PCL sheets (Osteopore International, Singapore). The scaffolds featured a honeycomb array of layers of interconnected struts oriented in a repeated lay-down pattern of 0°/60°/120°. Scaffolds were sterilized by ethanol evaporation and then soaked in a 50 μg/ml solution of the collagen-mimetic peptide GFOGER overnight at 4°C; the peptide has been shown to interact with the α2β1 integrin on stem cell surfaces and can induce osteoblast differentiation and enhance matrix mineralization (Reyes and Garcia 2003, 2004; Reyes et al. 2007). Next, scaffolds were coated with 1.5 mg/ml type I collagen (Vitrogen 100, Cohesion Technologies, Palo Alto, Calif., USA) through lyophilization to increase cell adhesion. Scaffolds were then placed in the wells of custom molds and coated with either 10^{10} particles of scAAV (McCarty et al. 2001) transcapsidated (2.5; Rabinowitz et al. 2004) vector expressing the human BMP2 gene (scAAV2.5-BMP2) or AAV-Luc (obtained from Vector Core Facility, University of North Carolina, Chapel Hill, N.C., USA) in 100 μl 1% sorbitol/phosphate-buffered saline (PBS) by lyophilization. The vector was prepared by using the helper-virus-free transfection method (Xiao et al. 1998), and the titer of DNA resistant viral particles was determined by dot blot assay such that the purified stocks were ~10^{12} particles/ml.

Two dimensional in vitro cell culture and AAV transduction

Human mesenchymal stem cells (MSCs) were obtained as a gift from Dr. Darwin Prockop at Tulane University (New Orleans, La., USA) and were originally isolated from bone marrow aspirates as described previously (Sekiya et al. 2002). Human amniotic fluid stem cells (AFS cells) were obtained as a gift from Dr. Anthony Atala and Dr. Shay Soker at the Wake Forest Institute for Regenerative Medicine (Winston-Salem, N.C., USA) and were originally isolated from human amniotic fluid as described previously (Delo et al. 2006; De Coppi et al. 2007); hAFS cells have been shown to be a potential alternative cell source for bone tissue engineering therapies, as they readily produce robust mineralized matrix within three-dimensional porous polymer scaffolds, both in vitro and ectopically in vivo (Peister et al. 2008, 2009).

Cells were seeded on tissue culture plates and grown in an incubator at 37°C/5% CO_2 in culture medium consisting of α-Minimum Essential Medium supplemented with 16.7% fetal bovine serum (Atlanta Biologicals, Lawrenceville, Ga., USA), 100 units/ml penicillin/100 μg/ml streptomycin/2 mM L-glutamine (Invitrogen, Carlsbad, Calif., USA). Cells were washed with PBS (Mediatech, Manassas, Va., USA) and then trypsinized, centrifuged, and resuspended; 20,000 hMSCs (passage 4) or hAFS cells (passage 19) were seeded onto 24-well plates and allowed to adhere for 24 h. A 1-ml droplet of culture medium was then added to one group of cells, whereas culture medium supplemented with the osteogenic supplements 10 mM β-glycerol phosphate and 50 μg/ml ascorbic acid 2-phosphate was added to the second group, culture medium/osteogenic supplements and AAV-Luc viral particles were added to the third group, and culture medium/osteogenic supplements and scAAV2.5-BMP2 viral particles were added to the fourth group (n=5 per group). For viral transduction, $0.5*10^9$ scAAV2.5-BMP2 or control AAV-Luc particles were added per well in 10 μl medium and gently agitated for AAV distribution, producing an initial estimated multiplicity of infection (MOI: ratio of number of viral particles to number of cells) of $2.5*10^4$. After 10 min, 1 ml medium was added per well, and plates were cultured at 37°C/5% CO_2 in an incubator. Media supernates were collected, and media were changed at days 2, 6, 9, 13, and 16. Supernate BMP2 levels were assessed by using an enzyme-linked immunosorbent assay (ELISA; BMP2-Quantikine kit, R&D Systems).

Cell lysates were collected at day 16 and used to determine DNA content by a PicoGreen DNA Assay (Quant-iT PicoGreen dsDNA Quantification Kit, Molecular Probes, Eugene, Ore., USA). The same lysates were used in an alkaline phosphatase (ALP) activity assay to assess osteogenic differentiation. The ALP substrate working solution was made by mixing equal parts of 20 mM p-nitrophenyl phosphate, 1.5 M 2-amino-2-methyl-1-propanol (pH 10.25), and 10 mM MgCl2. The experimental samples were mixed with the freshly made substrate working solution and incubated for 1 h at 37°C. The reaction was stopped by adding 1 N NaOH, and the absorbance was measured at 405 nm on a plate reader (PowerWave XS, Biotek, Vt., USA). All samples were run in triplicate and compared with p-nitrophenol standards.

To assess viral particle dose on transduction efficiency, hMSCs (passage 4) were cultured on 6-well plates at a density of 2000 cells/cm^2 (total cells=19,200/well) in culture medium. After 24 h, either $5*10^8$ (1× dose) or 10^9 (2× dose) AAV-LacZ (reporter gene that encodes for β-galactosidase) viral particles in 100 μl PBS were added to the cells in either 3 ml culture medium (High transduction volume) or in 500 μl culture medium followed by addition of 2.5 ml medium after 3 h (low transduction volume; *n*=3 per dose per transduction volume). After 3 or 6 days, cells were fixed in 0.2% glutaraldehyde and stained with X-Gal for 10 h followed by counterstaining with Nuclear Fast Red for 60 s. X-Gal-positive cells were counted, and total cell numbers were calculated by 4,6-diamidino-2-phenylindole (DAPI) staining of cell nuclei and fluorescence microscopy image analysis by using ImageJ software (NIH). hMSCs were also cultured in wells of an additional 6-well plate, and after 24 h, cells were fixed in 0.2% glutaraldehyde and stained with 5 ng/ml DAPI, followed by the counting of cell nuclei in order to quantify the initial number of cells present at the time of infection (*n*=3) to quantify the transduction efficiency.

Three-dimensional in vitro cell culture and AAV transduction

Three-dimensional in vitro study—One million hMSCs or hAFS cells in 100 μl culture medium were seeded on PCL scaffolds previously coated with 10^{10} lyophilized AAV particles for an initial MOI of 10^4. Each scaffold was located in one well of a 12-well tissue culture plate and was held with its long axis upright by a custom polymer/stainless steel stand. After a 75-min incubation, 5 ml culture medium supplemented with osteogenic supplements (10 mM β-glycerol phosphate and 50 μg/ml ascorbic acid 2-phosphate) was added to each well, covering each scaffold in its entirety. After 3 days of static culture, 12-well plates containing scaffolds were placed on a rocker plate (The Belly Button, Stovall Life Science, Greensboro, N.C., USA) to create dynamic culture conditions and were incubated for 12 weeks. Media supernates were collected, and media were changed every 3 days for 11 weeks (*n*=5 per cell type per AAV gene). Supernate BMP2 levels were assessed by using an ELISA assay.

Segmental defect study—Three million hMSCs were seeded on PCL scaffolds previously coated with 10^{10} lyophilized scAAV2.5-BMP2 or AAV-Luc particles at an initial MOI of $0.333*10^4$. Cells were seeded on scaffolds in 100 μl culture medium, and after 75 min, 4 ml culture medium was added to each well of the 12-well plates in which the scaffolds were held. Scaffolds were then cultured statically for 2 days prior to in vivo implantation.

Assessment of in vitro cell viability/DNA analysis

Viability of cells in the three-dimensional in vitro experiment was assessed at 12 weeks after seeding stem cells on scaffolds. One scaffold per group was cut in half longitudinally and then stained with Live/Dead stain (Molecular Probes). Scaffold images were obtained by using an Axio Observer inverted microscope (Carl Zeiss, Thornwood, NY). Images were

viewed at locations around the periphery, top, bottom, and central cut scaffold faces. Scaffolds chosen for viability assessment displayed the average mineral volume per group at the 12-week time point, as assessed by micro-CT scanning (discussed below).

The remaining four scaffolds per group were used to quantify DNA levels by using a PicoGreen Assay (QuantiT PicoGreen dsDNA Quantification Kit, Molecular Probes) following the manufacturer's protocol. Fluorescence was measured by using a fluorescence plate reader (PerkinElmer HTS 7000) at an excitation of 485 nm and emission of 535 nm. All samples were run in triplicate. Cell lysates from 24-well plates in the two-dimensional AAV-Luc/scAAV2.5-BMP2 study were collected after 16 days, and DNAwas extracted into PBS by freeze-thaw cycles and repeated vortexing of sample tubes. DNA levels were measured by the PicoGreen assay (n=5/group).

Segmental defect surgical technique

All surgical techniques were approved by the Georgia Institute of Technology Institute Animal Care and Use Committee (protocol A08066). Female immunocompromised athymic nude rats (Charles River Labs, Wilmington, Mass., USA), age 13 weeks, were anesthetized by using isoflurane. Bilateral full-thickness diaphyseal segmental defects, critically sized at 8 mm, were created and stabilized by using custom internal fixation plates, as described previously (Oest et al. 2007; Rai et al. 2007). These defects are particularly challenging in comparison with those employed by other groups, which have used rat femoral defects of 5-mm lengths or less in both immunocompetent (Yasko et al. 1992; Lee et al. 1994; Betz et al. 2006) and immunocompromised (Jager et al. 2007) rats. Defects were press-fit with one of four constructs as shown in Table 1. Constructs included PCL scaffold coated with scAAV2.5-BMP2 or AAV-Luc as a control (in vivo gene therapy: a variety of local host cells could be transduced) or PCL scaffold coated with scAAV2.5-BMP2 or AAV-Luc pre-seeded with three million hMSCs (ex vivo gene therapy: specifically selected cells are transduced, here hMSCs). Rats were given subcutaneous injections of 0.03 mg/kg buprenorphine every 8 h for the first 48 h post-surgery, and 0.01 mg/kg buprenorphine every 8 h for the following 24 h for pain relief.

Radiograph/micro-CT imaging

Three-dimensional in vitro study—In vitro mineral formation on three-dimensional scaffolds was measured by micro-CT scans at 3, 6, 9, and 12 weeks after stem cell seeding. Cell/scaffold constructs were sealed in custom sterile containers and scanned by micro-CT (Viva-CT 40, Scanco Medical, Bassersdorf, Switzerland). A 38.5-micron voxel resolution, 55-kVP voltage, and 109-μA current were used together with a Gaussian filter (sigma=1.2, support=1) to suppress noise, and a density threshold corresponding to 180.52 mg hydroxyapatite/cm^3 was used to discriminate newly formed mineral from polymer scaffolds.

Segmental defect study—Qualitative bone growth into defect sites was assessed by two-dimensional in vivo digital X-rays (Faxitron MX-20 Digital, Faxitron X-ray, Wheeling, Ill., USA) taken at 4, 8, and 12 weeks post-surgery after rats were anesthetized with isoflurane. Mineral formation in segmental defects was measured by micro-CT scans performed in vivo at 4, 8, and 12 weeks post-surgery and in post mortem scans. After application of isoflurane anesthesia, the sedated rats were positioned in a custom scanning chamber to isolate the defects in the center of the scanning region. In vivo scan parameters were similar to three-dimensional in vitro scan parameters; however, a density threshold corresponding to 272 mg hydroxyapatite/cm^3 was used to discriminate bone from soft tissues and polymer. A cylindrical volume of interest (VOI) of 4 1/3 mm in length centered at the middle of the defect region was chosen to ensure measurement of new in vivo mineral formation and to avoid the measurement of native cortical bone ends. Post mortem scans

were performed on extracted femurs from the same animals with a higher density threshold corresponding to 385 mg hydroxyapatite/cm^3 to account for denser and more mature bone than in the earlier in vivo scans. Sample sizes are shown in Table 1.

Biomechanical testing

Biomechanical torsional tests were performed on explanted femurs taken from rats sacrificed at 12 weeks post-surgery, as described previously (Oest et al. 2007; Rai et al. 2007). Briefly, samples were potted in Wood's metal (Alfa Aesar, Ward Hill, Mass., USA) and tested in torsion to failure at 3°/s on an ELF 3200 testing system (Bose EnduraTEC, Minnetonka, Minn., USA). Sample sizes are shown in Table 1.

Data analysis

Data were analyzed by using GraphPad Prism 5 software (GraphPad Software, La Jolla, Calif., USA). Analyses comparing three or more groups were analyzed by using an analysis of variance (ANOVA) with Tukey post hoc analyses for pairwise comparisons. Comparisons of two groups were analyzed by using unpaired *t*-tests. Whenever required, the raw data was transformed by using a natural logarithmic transformation to make the data normal and the variance independent of the mean (Kutner et al. 2005) prior to statistical analysis. If after transformation, the data comparing three or more groups was still not normal or the variance not independent of the mean, data sets were analyzed by using the Kruskal-Wallis non-parametric test followed by Dunn's multiple comparison test. For the comparisons of in vitro BMP2 release over time, a repeated measures ANOVA was performed with Bonferroni post tests. For the in vivo segmental defect study comparing treatment with the scAAV2.5-BMP2 scaffold with or without hMSCs and AAV-Luc scaffold with or without hMSCs, no significant differences were found between the two scAAV2.5-BMP2 groups or two AAV-Luc groups so they were each pooled to increase sample size. If after natural logarithmic transformation the pooled data variance was still not independent of the mean, Welch's correction for unequal variances was used in the unpaired *t*-test. Data are presented as mean±standard error of mean (SEM). A *P*-value of <0.05 was considered statistically significant.

Results

Two-dimensional in vitro AAV-LacZ transduction efficiency

Results of the two-dimensional in vitro viral dose study revealed the presence of blue β-galactosidase-expressing cells in all wells at both 3 and 6 days post-transduction (Fig. 1a, b), signifying successful transduction of hMSCs by AAV-LacZ. Transduction efficiency was determined as the ratio of blue cells to total cells; the latter were counted in fluorescence microscopy images (after cells had been treated with a DAPI nuclear stain) by using the software program ImageJ (Fig. 1c).

Transduction efficiency increased with viral dose and with lower medium volumes containing the viral particles, possibly because of better colocalization of the viral particles with the hMSCs (Fig. 2). Transduction efficiency also increased from day 3 to day 6, possibly because of a peak or jump in AAV transgene expression. The only significant differences in transduction efficiency were observed between the low transduction medium volume/2× AAV dose group at day 6 and the high transduction medium volume/1× AAV dose group at both days 3 and 6, perhaps attributable to the extremely small samples sizes (n=3). The average initial number of cells calculated in wells at 24 h after seeding was 24,321 per well, giving initial transduction multiplicity of infections of approximately $2*10^4$ and $4*10^4$.

Two-dimensional in vitro scAAV2.5-BMP2 stem cell transduction/osteogenic differentiation

Media samples taken from wells containing hMSCs transduced with scAAV2.5-BMP2 displayed significantly higher BMP2 concentrations than those from wells containing hMSCs or hAFS cells transduced with AAV-Luc (control) throughout the duration of the 16-day study (Fig. 3a). By day 6, medium from scAAV2.5-BMP2-transduced hMSCs displayed peak BMP2 concentration, which was also significantly higher than that of scAAV2.5-BMP2-transduced hAFS cells, and this continued throughout the rest of the study. scAAV2.5-BMP2 transduction of hAFS cells failed to cause an increase in BMP2 concentration in media samples during the 16-day experiment.

After 16 days, ALP expression in cell lysates was measured in order to assess osteogenic differentiation of stem cells. An endpoint of 16 days was chosen based upon preliminary studies showing a peak in transient ALP expression from scAAV2.5-BMP2-transduced cells at that time point (data not shown). ALP activity in hMSCs transduced with scAAV2.5-BMP2 was significantly higher than in hMSCs and hAFS cells cultured in non-osteogenic medium (Fig. 3b). When ALP levels were normalized by DNA content, scAAV2.5-BMP2-transduced hMSC levels were significantly higher than that in all other groups (Fig. 3d). scAAV2.5-BMP2 transduction of hAFS cells failed to cause an increase in ALP activity in cell lysates during the 16-day experiment. Cells cultured in osteogenic medium in the absence of scAAV2.5-BMP2 failed to experience any significant increases in ALP activity, most likely because of the lack of dexamethasone, a potent stimulator of stem cell osteogenic differentiation, in the medium. hAFS cell DNA levels were significantly higher than hMSC DNA levels in all media condition groups, suggesting increased cell proliferation of hAFS cells compared with hMSCs (Fig. 3c). Of particular importance was a significantly reduced DNA content in scAAV2.5-BMP2-transduced hMSCs compared with all other groups, suggesting reduced stem cell proliferation attributable to increased osteogenic differentiation.

Three-dimensional in vitro scAAV2.5-BMP2 stem cell transduction/osteogenic differentiation

BMP2 concentrations in media samples from wells containing hMSCs seeded on scAAV2.5-BMP2-coated scaffolds displayed an expression pattern similar to that in the two-dimensional experiment, with a peak at 1 week after transduction (Fig. 4). Interestingly, BMP2 concentrations from wells containing hAFS cells seeded on scAAV2.5-BMP2-coated scaffolds significantly increased above levels in all other groups but not until 7 weeks after transduction, and the BMP2 peak was nearly twice as high (7788.74 versus 4811.82 pg/ml) and lasted for three times as long (days 44–65 versus days 4–11) in hAFS cells compared with hMSCs.

Mineral formation in hMSC-seeded/scAAV2.5-BMP2-coated scaffolds was significantly higher than in hMSC-seeded/AAV-Luc coated scaffolds and hAFS cell-seeded/scAAV2.5-BMP2-coated scaffolds beginning at week 6 and continuing through weeks 9 and 12 (Fig. 5a–e). The lack of significant differences at week 3 suggests a delay in osteogenic differentiation, or at least in resulting mineral formation, after BMP2 expression, which peaked at day 7. Whereas BMP2 expression in hAFS cell-seeded/scAAV2.5-BMP2-coated scaffolds significantly increased after 7 weeks, no resulting increase in mineral formation occurred by week 12 of the study.

Live cells were observed throughout scaffolds from each group at week 12 (Fig. 5f). Such cells were found along the outer periphery of the cylindrical scaffolds, along the surface of a longitudinally cut cross section, and on both the top and bottom surfaces of the scaffolds. As in the two-dimensional in vitro study, DNA content of scaffolds seeded with hMSCs

transduced with scAAV2.5-BMP2 was significantly lower than scaffolds seeded with hMSCs transduced with AAV-Luc (Fig. 6), again probably attributable to increased stem cell differentiation resulting in reduced stem cell proliferation.

Critically sized nude rat femoral defect study

By 12 weeks post-surgery, bony bridging occurred in 5/10 defects treated with scAAV2.5-BMP2-coated scaffolds alone, 3/10 defects treated with scAAV2.5-BMP2-coated scaffolds seeded with hMSCs pre-implantation, 1/6 defects treated with AAV-Luc-coated scaffolds alone, and 0/8 defects treated with AAV-Luc-coated scaffolds seeded with hMSCs pre-implantation. Notably, mineral formation was restricted to the immediate vicinity of the segmental defect site, suggesting that BMP2 delivery via scAAV2.5-BMP2-coated polymer scaffolds avoided the ectopic bone formation that can be associated with bolus delivery of large doses of recombinant BMP2. Representative defect mineral formation in each group is shown in Fig. 7, both in radiographic images from weeks 4 and 12 and in corresponding week 12 micro-CT images.

Quantitative comparison of micro-CT-measured mineral volumes revealed significantly higher mineral formation in the scAAV2.5-BMP2-coated scaffold treatment group compared with the AAV-Luc-coated scaffold treatment group and the hMSC pre-seeded AAV-Luc scaffold treatment groups at week 8 in vivo and in post mortem scans (Fig. 8a, b). A significant difference in mineral volume existed between the scAAV2.5-BMP2 scaffold treatment group and the hMSC pre-seeded AAV-Luc scaffold group at week 12. Biomechanical torsional testing revealed significantly higher maximum torque and torsional stiffness in the scAAV2.5-BMP2 scaffold treatment group compared with the hMSC pre-seeded AAV-Luc scaffold treatment group (Fig. 8c, d).

Comparison of pooled scAAV2.5-BMP2 therapies with pooled AAV-Luc therapies showed significant differences in both in vivo and post mortem mineral volumes (Fig. 9a, b) and in maximum torque and torsional stiffness (Fig. 9c, d).

Discussion

This study presents evidence that synthetic polymer scaffolds can be functionalized for applications in the repair of critically sized bone defects through lyophilization of scAAV encoding the gene for human BMP2. Traditional AAV has inefficient transgene expression because of the need for replication of the single-stranded DNA genome prior to transgene expression; however, the modified scAAV features self-complementary DNA strands, increasing the efficiency of transgene expression in MSCs (Yazici et al. 2011; Kim et al. 2007). The in vitro BMP2 release kinetics have shown that transduced marrow-derived stem cells exhibit peak BMP2 release after 1 week in both two-dimensional and three-dimensional culture, whereas amniotic-fluid-derived cells exhibit a delay of nearly 2 months before achieving significant BMP2 expression in three-dimensional culture. The hMSC peak release profile might be advantageous for bone healing as it may coincide with the end of the inflammatory phase of the long-bone-injury response, during which a variety of signals are present, and the initiation of the reparative phase of healing (Yazici et al. 2008). Furthermore, the extended BMP2 expression continues through at least 5 weeks for both stem cell types in three-dimensional culture.

The BMP2 expressed by transduced hMSCs leads to increases in both two-dimensional and three-dimensional osteogenic outcomes, as assessed by increased ALP levels per DNA and increased mineral volumes per scaffold, respectively. The increased osteogenic differentiation also likely results in reduced cell numbers as determined by DNA analysis, because differentiated cells are less proliferative. No increase in mineral volume has been

found in scAAV2.5-BMP2-transduced hAFS cell three-dimensional constructs after 12 weeks. The fetal-derived hAFS cells might be more developmentally primitive than the adult-derived hMSCs, and transduction efficiency differences between the two cell types (possibly attributable to differences in AAV receptor numbers or activities) might have been responsible for the observed differences in BMP2 secretion kinetics between the two cell sources. After 12 weeks in three-dimensional culture, the AAV-Luc-transduced hAFS cells promote greater mineralizaton than the scAAV2.5-BMP2-expressing hAFS cells, suggesting that BMP2 transduction might be counterproductive for the promotion of mineral formation by these cells, or that the cells might not have responded to the scAAV2.5-BMP2 within the duration of the 12-week study.

The in vivo results have revealed that a AAV coating of PCL porous polymer scaffolds by lyophilization can serve as a successful vehicle for delivering genes to large bone defects in order to enhance endogenous repair. This study has shown that the direct delivery of scAAV2.5-BMP2-coated scaffolds to defect sites (in vivo gene therapy) leads to more defect bridging than does the delivery of scAAV2.5-BMP2-coated scaffolds pre-seeded with hMSCs before implantation (ex vivo gene therapy). Segmental defects treated by in vivo delivery of scAAV2.5-BMP2-coated scaffolds display significantly higher mineral volumes, maximum torque, and torsional stiffness at in vivo week 8, in vivo week 12, and post mortem, compared with defects treated with AAV-Luc-coated scaffolds pre-seeded with hMSCs. Defects treated with scAAV2.5-BMP2-coated scaffolds also display significantly higher mineral volumes at in vivo week 8 and post mortem compared with defects treated with AAV-Luc-coated scaffolds, although no significant differences have been seen in mineral volumes or biomechanical properties at in vivo week 12, possibly in part because of the smaller sample size of the group (n=6), compared with AAV-Luc-coated scaffold pre-seeded with hMSCs (n=8). When in vivo and ex vivo gene therapy data are pooled, defect treatment by scAAV2.5-BMP2 leads to significantly higher in vivo and post mortem mineral formation at all time points and to enhanced biomechanical properties compared with defects treated by AAV-Luc.

The results of the in vivo study have refuted our initial hypothesis that the addition of stem cells while treating defects with scaffolds providing osteogenic signals would enhance bone repair. The lack of stem-cell-mediated repair might be attributable to a variety of factors. One primary factor might be the variability in scAAV2.5-BMP2 transduction and BMP2 expression in the different cell types, as the implanted hMSCs would have taken up the virus, which otherwise would have been available to transduce potentially more robust endogenous cells. Additionally, the hMSCs might have experienced limited viability after delivery, thus decreasing secreted BMP2 levels. For therapies incorporating stem cells, a key element in maintaining cell viability is the rapid development of a vascular network throughout the scaffold to provide cells with oxygen and nutrients crucial to their survival (Meijer et al. 2007). Co-delivery of angiogenic cues such as provided by vascular endothelial growth factor (VEGF) could enhance this development. Direct injection of an AAV vector delivering the genes for both BMP7 and VEGF increases angiopoiesis and bone regeneration in a rabbit hindlimb ischemia model over delivery of AAV encoding either gene alone (Zhang et al. 2010), and i.v. injection of MSCs transduced with rAAV-BMP6 and rAAV-VEGF enhances the healing of tibial defects in nude mice (Kumar et al. 2010). Coating scaffolds with the genes encoding both BMP2 and VEGF could lead to a similar enhancement of segmental defect repair by scaffolds pre-seeded with hMSCs by promoting prolonged cell viability, thus extending the potential duration for BMP2 release.

Other possible explanations for the differences in defect repair between acellular scaffolds and scaffolds pre-seeded with hMSCs include differences in the amount of time that cells are directly exposed to the scAAV2.5-BMP2 vector, loss of AAV particles from scaffolds

into the surrounding media in culture prior to implantation, or migration of hMSCs from defect sites. Furthermore, stem cells transduced with AAV prior to implantation might have experienced an increased immune response upon delivery compared with acellular scaffolds; whereas nude rats are T-cell-deficient, their immune systems still have other lymphocytes, such as natural killer cells and B cells that might have responded to the implanted xenogeneic human cells. However, delivered human stem cells are unlikely to have elicited a strong immune response, as multiple groups have reported that MSCs are possibly immune-privileged (Arinzeh et al. 2003; Le Blanc and Ringden 2006; Zhang et al. 2007). The delivered human stem cells might also have deterred the endogenous cell response, either from host osteoprogenitors or osteogenic cells. During the normal bone repair process, host stem cells would occupy the injury site and differentiate into bone-forming cells, but in this study, the defects are occupied by the delivered cells, possibly limiting the endogenous cellular response. Finally, transduction of host cells by AAV delivered on acellular scaffolds might have occurred at a later time point when the initial inflammatory stage of bone repair is subsiding and a more hospitable immune environment is present. Combined, these results suggest that, compared with the delivery of scaffolds pre-seeded with stem cells, defect therapy by acellular scAAV2.5-BMP2-coated PCL scaffolds presents a simpler and more effective treatment that stimulates an enhanced healing response of host endogenous cell populations.

Defect healing might be further increased by using a higher dose of viral particles. Yazici et al. (2011) have reported that the delivery of 10^{10} scAAV-BMP2 particles coated onto 4-mm murine allografts to murine femoral defects results in functional defect healing superior to autograft treatment, whereas lower particle doses fail to provide an efficacious repair response. A greater number of particles might be necessary for functional repair of larger 8-mm rat femoral defects. Increasing AAV particle dose contributes to in vitro increases in transduction efficiency, as shown in Fig. 2. Coating scaffolds with a higher number of viral particles would likely increase the number of cells transduced and lead to increased BMP2 production. Increased BMP2 expression could in turn lead to more robust mineral formation, more bridged defects, and the full restoration of femoral biomechanical function.

In conclusion, this study presents evidence of a novel acellular bone-graft-free tissue-engineering therapy for stimulating endogenous repair mechanisms, with the potential for off-the-shelf clinical application. In this treatment method, biodegradable porous polymer scaffolds of variable sizes could be coated by thermostable lyophilized scAAV2.5-BMP2 and then frozen until needed for clinical implantation into large-bone-defect sites.

Acknowledgments

The authors thank Angela Lin, Mela Johnson, Chris Dosier, Jessica O'Neal Green, Jason Wang, Laura O'Farrell, Alex Peister, and Brent Uhrig for additional assitance during these studies, and Andres Garcia for providing GFOGER.

Funding was provided by National Institutes of Health Grant R01 AR051336 and PHS Awards DE19902/AR54041 and by a Musculoskeletal Transplant Foundation grant.

References

Arinzeh TL, Peter SJ, Archambault MP, Bos C, van den Gordon S, Kraus K, Smith A, Kadiyala S. Allogeneic mesenchymal stem cells regenerate bone in a critical-sized canine segmental defect. J Bone Joint Surg Am. 2003; 85-A:1927–1935. [PubMed: 14563800]

Awad HA, Zhang X, Reynolds DG, Guldberg RE, O'Keefe RJ, Schwarz EM. Recent advances in gene delivery for structural bone allografts. Tissue Eng. 2007; 13:1973–1985. [PubMed: 17518728]

Berrey BH Jr, Lord CF, Gebhardt MC, Mankin HJ. Fractures of allografts. Frequency, treatment, and end-results. J Bone Joint Surg Am. 1990; 72:825–833. [PubMed: 2365716]

Betz OB, Betz VM, Nazarian A, Pilapil CG, Vrahas MS, Bouxsein ML, Gerstenfeld LC, Einhorn TA, Evans CH. Direct percutaneous gene delivery to enhance healing of segmental bone defects. J Bone Joint Surg Am. 2006; 88:355–365. [PubMed: 16452748]

Bucholz RW. Nonallograft osteoconductive bone graft substitutes. Clin Orthop Relat Res. 2002; 395:44–52. [PubMed: 11937865]

Burastero G, Scarfi S, Ferraris C, Fresia C, Sessarego N, Fruscione F, Monetti F, Scarfo F, Schupbach P, Podesta M, Grappiolo G, Zocchi E. The association of human mesenchymal stem cells with BMP-7 improves bone regeneration of critical-size segmental bone defects in athymic rats. Bone. 2010; 47:117–126. [PubMed: 20362702]

Cahill KS, Chi JH, Day A, Claus EB. Prevalence, complications, and hospital charges associated with use of bone-morphogenetic proteins in spinal fusion procedures. JAMA. 2009; 302:58–66. [PubMed: 19567440]

Chen D, Zhao M, Mundy GR. Bone morphogenetic proteins. Growth Factors. 2004; 22:233–241. [PubMed: 15621726]

De Coppi P, Bartsch G Jr, Siddiqui MM, Xu T, Santos CC, Perin L, Mostoslavsky G, Serre AC, Snyder EY, Yoo JJ, Furth ME, Soker S, Atala A. Isolation of amniotic stem cell lines with potential for therapy. Nat Biotechnol. 2007; 25:100–106. [PubMed: 17206138]

Delo DM, De Coppi P, Bartsch G Jr, Atala A. Amniotic fluid and placental stem cells. Methods Enzymol. 2006; 419:426–438. [PubMed: 17141065]

Dupont KM, Sharma K, Stevens HY, Boerckel JD, Garcia AJ, Guldberg RE. Human stem cell delivery for treatment of large segmental bone defects. Proc Natl Acad Sci USA. 2010; 107:3305–3310. [PubMed: 20133731]

Einhorn TA. Clinical applications of recombinant human BMPs: early experience and future development. J Bone Joint Surg Am. 2003; 85-A(Suppl 3):82–88. [PubMed: 12925614]

Hutmacher DW. Scaffolds in tissue engineering bone and cartilage. Biomaterials. 2000; 21:1169–1185.

Ito H, Koefoed M, Tiyapatanaputi P, Gromov K, Goater JJ, Carmouche J, Zhang X, Rubery PT, Rabinowitz J, Samulski RJ, Nakamura T, Soballe K, O'Keefe RJ, Boyce BF, Schwarz EM. Remodeling of cortical bone allografts mediated by adherent rAAV-RANKL and VEGF gene therapy. Nat Med. 2005; 11:291–297. [PubMed: 15711561]

Jager M, Degistirici O, Knipper A, Fischer J, Sager M, Krauspe R. Bone healing and migration of cord blood-derived stem cells into a critical size femoral defect after xenotransplantation. J Bone Miner Res. 2007; 22:1224–1233. [PubMed: 17451370]

Kalfas IH. Principles of bone healing. Neurosurg Focus. 2001; 10:E1. [PubMed: 16732625]

Kim SJ, Lee WI, Heo H, Shin O, Kwon YK, Lee H. Stable gene expression by self-complementary adeno-associated viruses in human MSCs. Biochem Biophys Res Commun. 2007; 360:573–579. [PubMed: 17606219]

Koefoed M, Ito H, Gromov K, Reynolds DG, Awad HA, Rubery PT, Ulrich-Vinther M, Soballe K, Guldberg RE, Lin AS, O'Keefe RJ, Zhang X, Schwarz EM. Biological effects of rAAV-caAlk2 coating on structural allograft healing. Mol Ther. 2005; 12:212–218. [PubMed: 16043092]

Kolambkar YM, Dupont KM, Boerckel JD, Huebsch N, Mooney DJ, Hutmacher DW, Guldberg RE. An alginate-based hybrid system for growth factor delivery in the functional repair of large bone defects. Biomaterials. 2010; 32:65–74. [PubMed: 20864165]

Kumar S, Wan C, Ramaswamy G, Clemens TL, Ponnazhagan S. Mesenchymal stem cells expressing osteogenic and angiogenic factors synergistically enhance bone formation in a mouse model of segmental bone defect. Mol Ther. 2010; 18:1026–1034. [PubMed: 20068549]

Kutner, MH.; Nachtsheim, CJ.; Neter, J.; Li, W. Applied linear statistical models. 5. McGraw-Hill; New York: 2005.

Le Blanc K, Ringden O. Mesenchymal stem cells: properties and role in clinical bone marrow transplantation. Curr Opin Immunol. 2006; 18:586–591. [PubMed: 16879957]

Lee SC, Shea M, Battle MA, Kozitza K, Ron E, Turek T, Schaub RG, Hayes WC. Healing of large segmental defects in rat femurs is aided by RhBMP-2 in PLGA matrix. J Biomed Mater Res. 1994; 28:1149–1156. [PubMed: 7829545]

McCarty DM, Monahan PE, Samulski RJ. Self-complementary recombinant adeno-associated virus (scAAV) vectors promote efficient transduction independently of DNA synthesis. Gene Ther. 2001; 8:1248–1254. [PubMed: 11509958]

Meijer GJ, Bruijn JD, de Koole R, van Blitterswijk CA. Cell-based bone tissue engineering. PLoS Med. 2007; 4:e9. [PubMed: 17311467]

Mroz TE, Joyce MJ, Steinmetz MP, Lieberman IH, Wang JC. Musculoskeletal allograft risks and recalls in the United States. J Am Acad Orthop Surg. 2008; 16:559–565. [PubMed: 18832599]

Oest ME, Dupont KM, Kong HJ, Mooney DJ, Guldberg RE. Quantitative assessment of scaffold and growth factor-mediated repair of critically sized bone defects. J Orthop Res. 2007; 25:941–950. [PubMed: 17415756]

Ohura K, Hamanishi C, Tanaka S, Matsuda N. Healing of segmental bone defects in rats induced by a beta-TCP-MCPM cement combined with rhBMP-2. J Biomed Mater Res. 1999; 44:168–175. [PubMed: 10397918]

Peister A, Porter BD, Kolambkar YM, Hutmacher DW, Guldberg RE. Osteogenic differentiation of amniotic fluid stem cells. Biomed Mater Eng. 2008; 18:241–246. [PubMed: 19065029]

Peister A, Deutsch ER, Kolambkar Y, Hutmacher DW, Guldberg R. Amniotic fluid stem cells produce robust mineral deposits on biodegradable scaffolds. Tissue Eng Part A. 2009; 15:3129–3138. [PubMed: 19344289]

Rabinowitz JE, Bowles DE, Faust SM, Ledford JG, Cunningham SE, Samulski RJ. Cross-dressing the virion: the transcapsidation of adeno-associated virus serotypes functionally defines subgroups. J Virol. 2004; 78:4421–4432. [PubMed: 15078923]

Rai B, Teoh SH, Ho KH, Hutmacher DW, Cao T, Chen F, Yacob K. The effect of rhBMP-2 on canine osteoblasts seeded onto 3D bioactive polycaprolactone scaffolds. Biomaterials. 2004; 25:5499–5506. [PubMed: 15142731]

Rai B, Oest ME, Dupont KM, Ho KH, Teoh SH, Guldberg RE. Combination of platelet-rich plasma with polycaprolactone-tricalcium phosphate scaffolds for segmental bone defect repair. J Biomed Mater Res A. 2007; 81:888–899. [PubMed: 17236215]

Reyes CD, Garcia AJ. Engineering integrin-specific surfaces with a triple-helical collagen-mimetic peptide. J Biomed Mater Res A. 2003; 65:511–523. [PubMed: 12761842]

Reyes CD, Garcia AJ. Alpha2beta1 integrin-specific collagen-mimetic surfaces supporting osteoblastic differentiation. J Biomed Mater Res A. 2004; 69:591–600. [PubMed: 15162400]

Reyes CD, Petrie TA, Burns KL, Schwartz Z, Garcia AJ. Biomolecular surface coating to enhance orthopaedic tissue healing and integration. Biomaterials. 2007; 28:3228–3235. [PubMed: 17448533]

Saito N, Murakami N, Takahashi J, Horiuchi H, Ota H, Kato H, Okada T, Nozaki K, Takaoka K. Synthetic biodegradable polymers as drug delivery systems for bone morphogenetic proteins. Adv Drug Deliv Rev. 2005; 57:1037–1048. [PubMed: 15876402]

Schwarz EM. The adeno-associated virus vector for orthopaedic gene therapy. Clin Orthop Relat Res. 2000; 379 (Suppl):S31–S39. [PubMed: 11039749]

Sekiya I, Larson BL, Smith JR, Pochampally R, Cui JG, Prockop DJ. Expansion of human adult stem cells from bone marrow stroma: conditions that maximize the yields of early progenitors and evaluate their quality. Stem Cells. 2002; 20:530–541. [PubMed: 12456961]

Tseng SS, Lee MA, Reddi AH. Nonunions and the potential of stem cells in fracture-healing. J Bone Joint Surg Am. 2008; 90 (Suppl 1):92–98. [PubMed: 18292363]

Werntz JR, Lane JM, Burstein AH, Justin R, Klein R, Tomin E. Qualitative and quantitative analysis of orthotopic bone regeneration by marrow. J Orthop Res. 1996; 14:85–93. [PubMed: 8618172]

Wojtowicz AM, Shekaran A, Oest ME, Dupont KM, Templeman KL, Hutmacher DW, Guldberg RE, Garcia AJ. Coating of biomaterial scaffolds with the collagen-mimetic peptide GFOGER for bone defect repair. Biomaterials. 2010; 31:2574–2582. [PubMed: 20056517]

Wozney JM, Rosen V. Bone morphogenetic protein and bone morphogenetic protein gene family in bone formation and repair. Clin Orthop Relat Res. 1998; 346:26–37. [PubMed: 9577407]

Xiao X, Li J, Samulski RJ. Production of high-titer recombinant adeno-associated virus vectors in the absence of helper adenovirus. J Virol. 1998; 72:2224–2232. [PubMed: 9499080]

Yasko AW, Lane JM, Fellinger EJ, Rosen V, Wozney JM, Wang EA. The healing of segmental bone defects, induced by recombinant human bone morphogenetic protein (rhBMP-2). A radiographic, histological, and biomechanical study in rats. J Bone Joint Surg Am. 1992; 74:659–670. [PubMed: 1378056]

Yazici C, Yanoso L, Xie C, Reynolds DG, Samulski RJ, Samulski J, Yannariello-Brown J, Gertzman AA, Zhang X, Awad HA, Schwarz EM. The effect of surface demineralization of cortical bone allograft on the properties of recombinant adeno-associated virus coating. Biomaterials. 2008; 29:3882–3887. [PubMed: 18590929]

Yazici C, Takahata M, Reynolds DG, Xie C, Samulski RJ, Samulski J, Beecham EJ, Gertzman AA, Spilker M, Zhang X, O'Keefe RJ, Awad HA, Schwarz EM. Self-complementary AAV2.5-BMP2-coated femoral allografts mediated superior bone healing versus live autografts in mice with equivalent biomechanics to unfractured femur. Mol Ther. 2011 (in press).

Younger EM, Chapman MW. Morbidity at bone graft donor sites. J Orthop Trauma. 1989; 3:192–195. [PubMed: 2809818]

Zhang W, Qin C, Zhou ZM. Mesenchymal stem cells modulate immune responses combined with cyclosporine in a rat renal transplantation model. Transplant Proc. 2007; 39:3404–3408. [PubMed: 18089393]

Zhang C, Wang KZ, Qiang H, Tang YL, Li Q, Li M, Dang XQ. Angiopoiesis and bone regeneration via co-expression of the hVEGF and hBMP genes from an adeno-associated viral vector in vitro and in vivo. Acta Pharmacol Sin. 2010; 31:821–830. [PubMed: 20581855]

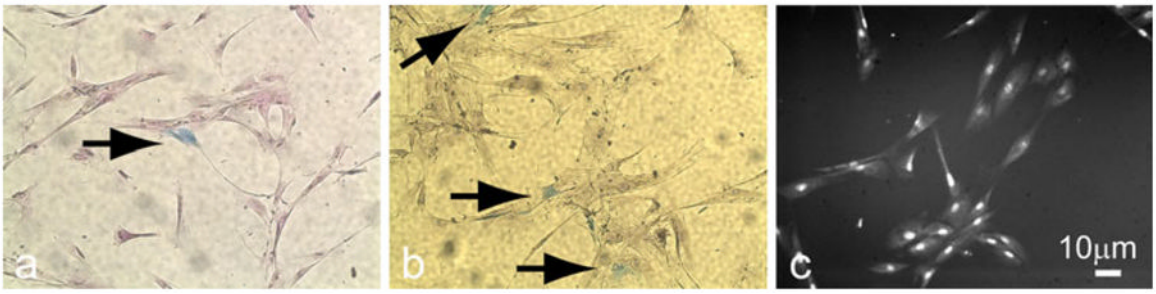

Fig. 1.

Two-dimensional in vitro transduction of human mesenchymal stem cells (hMSCs) by adeno-associated viral vector (AAV)-LacZ (reporter gene that encodes for β-galactosidase). **a**, **b** Expression of β-galactosidase (*blue*) in hMSC at 3 or 6 days, respectively, after viral transduction (*arrows* transduced cells). **c** DAPI (4,6-diamidino-2-phenylindole)-stained cell nuclei used to estimate total cell number

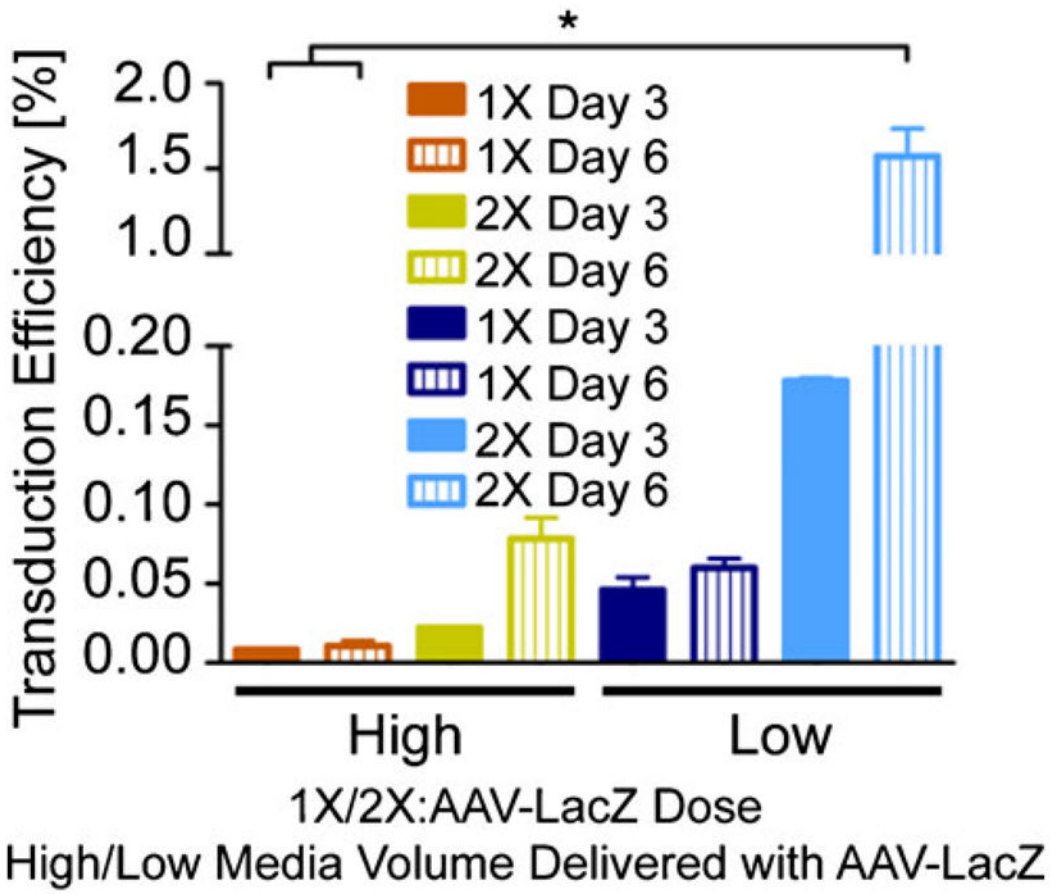

Fig. 2.
Effects of viral dose and transduction medium volume on AAV-LacZ transduction efficiency

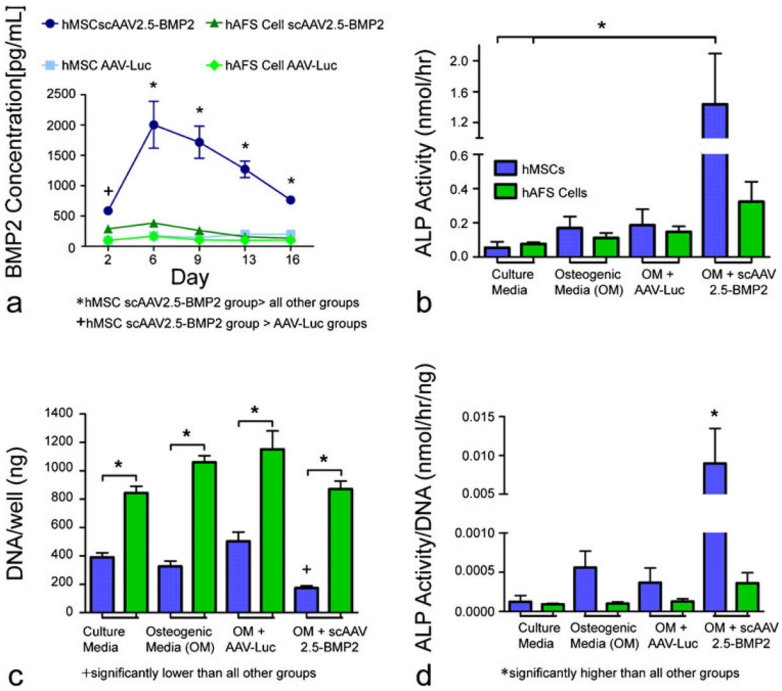

Fig. 3.

Two-dimensional in vitro evidence of scAAV2.5-BMP2 (bone morphogenetic protein 2) transduction of hMSCs resulting in an increase in osteogenic differentiation. **a** BMP2 concentrations in harvested media samples from wells containing stem cells in osteogenic medium after day-0 transduction with scAAV2.5-BMP2 or AAV-Luc. **b** Alkaline phosphatase (*ALP*) activity measured in cell lysates collected 16 days after transduction by AAV-Luc or scAAV2.5-BMP2. **c** DNA levels measured from cell lysates. **d** ALP activity normalized by DNA level per well. *,^{+}P<0.05

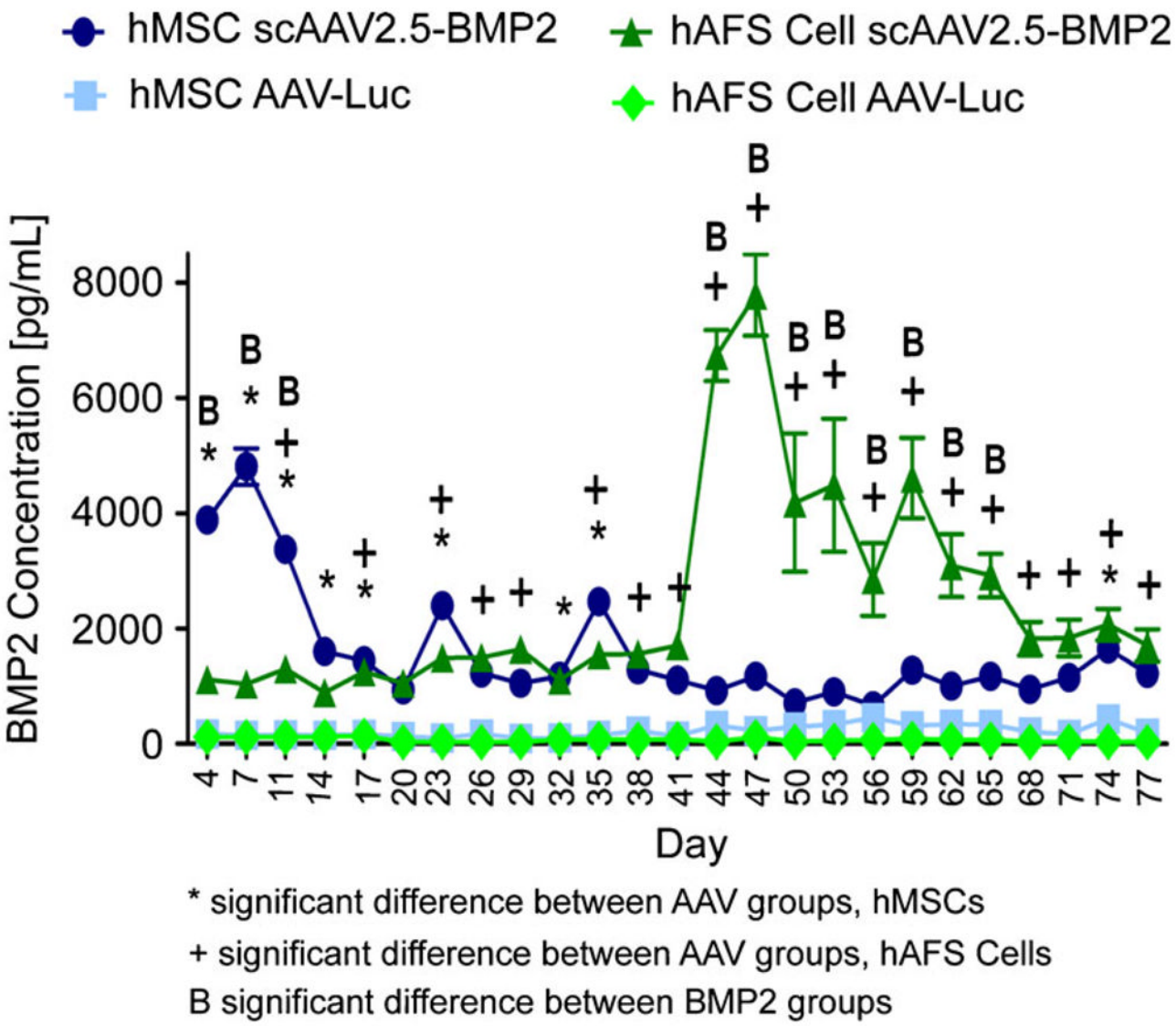

Fig. 4.

Three-dimensional in vitro evidence of scAAV2.5-BMP2 transduction of hMSCs and hAFS cells. BMP2 concentrations in harvested media samples from wells containing stem cells seeded on PCL scaffolds previously coated by scAAV2.5-BMP2 or AAV-Luc lyophilization. $^{*,+,B}P<0.05$

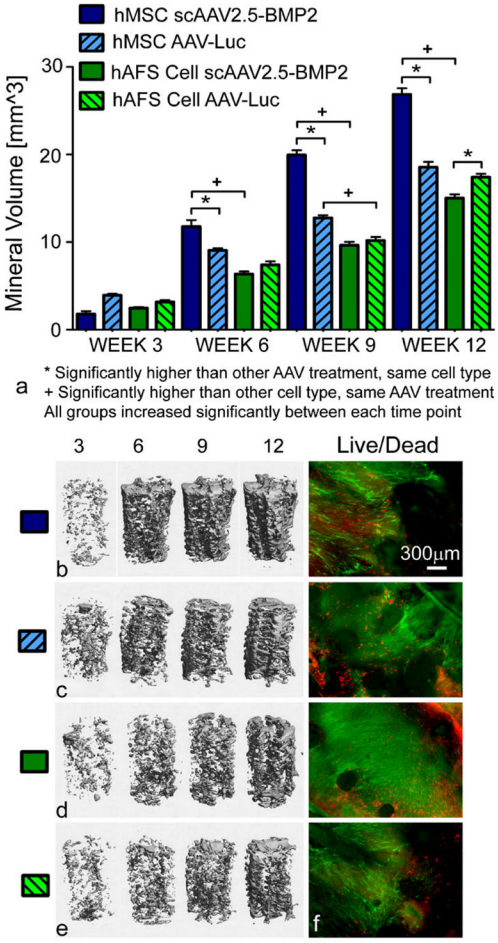

Fig. 5.

Evaluation of osteogenic differentiation of stem cells seeded on three-dimensional PCL scaffolds previously coated with lyophilized AAV. **a** Quantitative comparison of mineral volumes within PCL scaffolds. *,^{+}P<0.05. **b–e** Representative micro-CT images of mineral formation within scaffolds. **f** Live/Dead microscopy images of scaffolds showing live *green* cells along the circumferential periphery of scaffolds (*red* dead cells). Images are shown at ×4 magnification

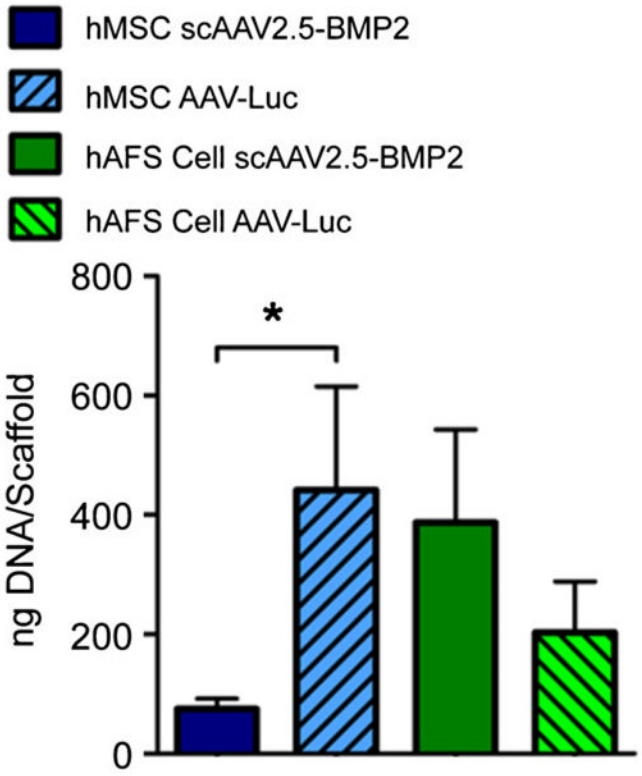

Fig. 6.
DNA per scaffold after 12 weeks in vitro culture. *P<0.05

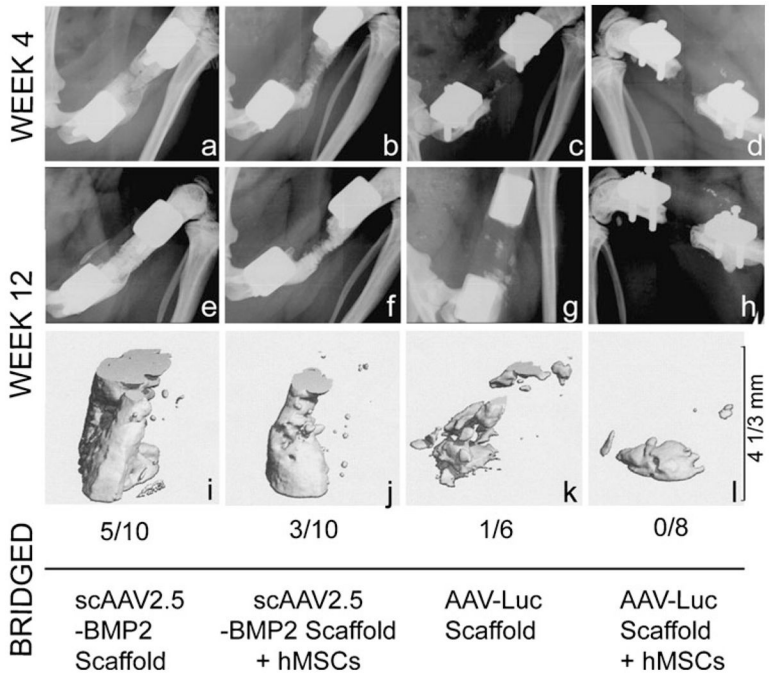

Fig. 7.

Qualitative mineral formation at the defect site after in vivo delivery of AAV-coated PCL scaffolds with or without pre-seeding of hMSCs. Radiographic (**a–h**) and in vivo micro-CT (**i–l**) images from defects that had the representative mineral formation per group, together with the bony bridging rate for each treatment group

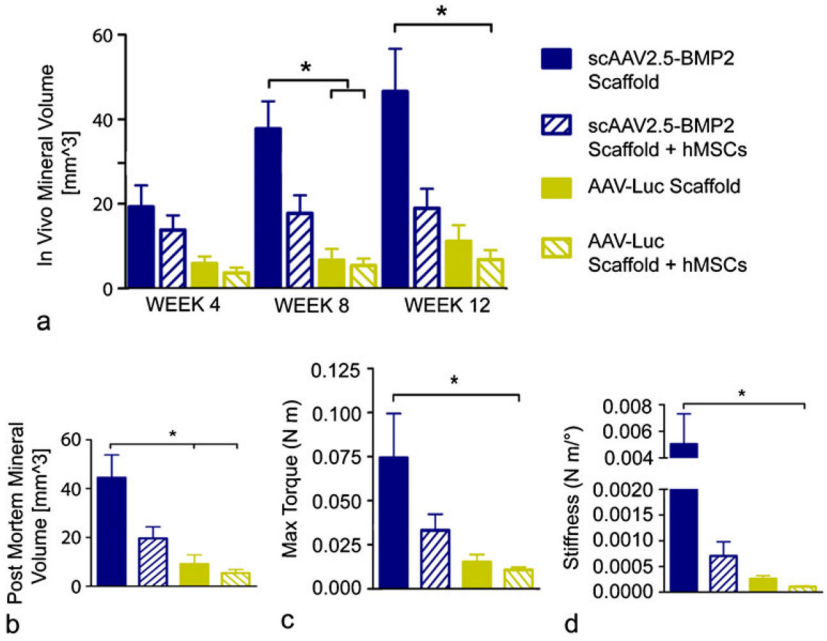

Fig. 8.

Quantitative structural and functional results from in vivo delivery of AAV-coated scaffolds with or without pre-seeding of hMSCs. **a** In vivo mineral volume within defect sites as obtained by micro-CT. **b** Post mortem mineral volume within defect sites as obtained by micro-CT. **c**, **d** Biomechanical properties of femurs tested to failure in torsion. **P*<0.05

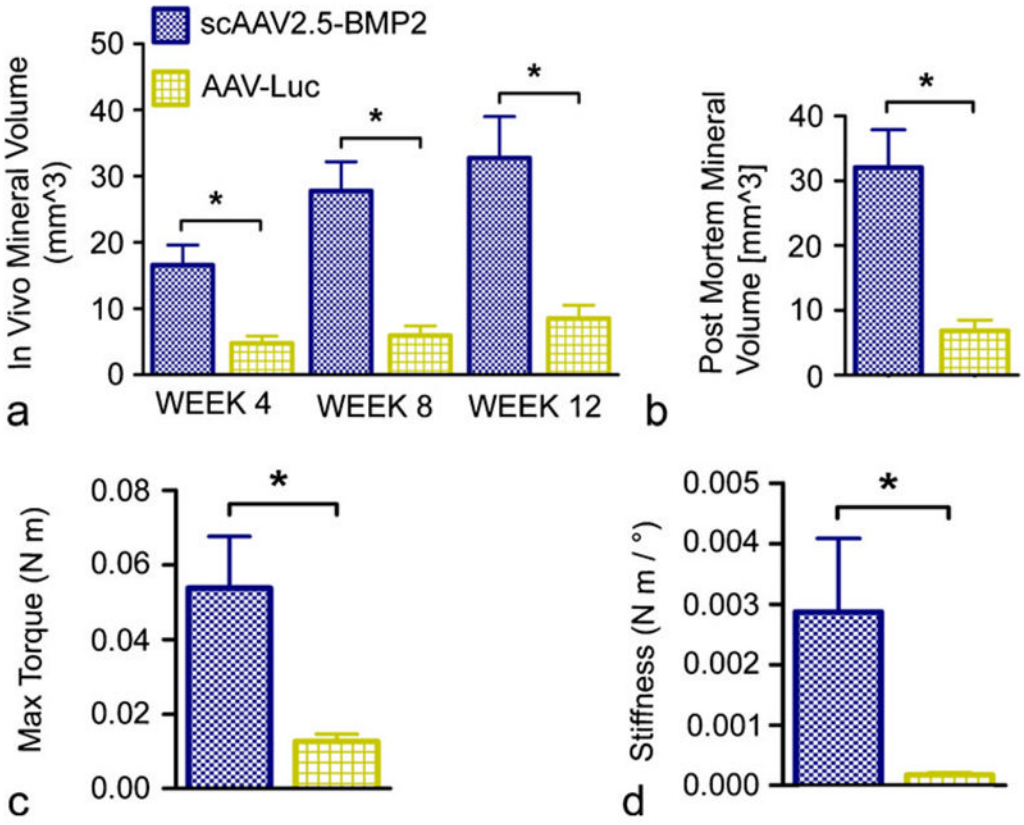

Fig. 9.

Quantitative comparison of structural and functional results from in vivo delivery of pooled scAAV2.5-BMP2 treatments or AAV-Luc treatments. **a**, **b** In vivo and post mortem mineral formation within defect sites. **c**, **d** Biomechanical properties of femurs tested to failure in torsion. *P<0.05

Table 1

Segmental defect study; groups and analyses performed

Treatment groups	Analysis methods and sample sizes		
	X-ray	Micro-CT	Mechanical test
scAAV2.5-BMP2-coated PCL scaffold	10	10	10
scAAV2.5-BMP2-coated PCL scaffold+3 million hMSCs	10	10	10
AAV-Luc-coated PCL scaffold	6	6	6
AAV-Luc-coated PCL scaffold+3 million hMSCs	8	8	8